



UDC 528.932.6

PERFORMANCE ASSESSMENT OF SPATIAL INTERPOLATIONS FOR TRAFFIC NOISE MAPPING ON UNDULATING AND LEVEL TERRAIN

 Nevil WICKRAMATHILAKA^{1,2}, Uznir UJANG¹, Suhaibah AZRI¹, Tan Liat CHOON¹
¹3D GIS Research Lab, Faculty of Built Environment and Surveying, Universiti Teknologi Malaysia, 81310, Johor Bahru, Johor, Malaysia

²Southern Campus, General Sir John Kotelawala Defence University, Edison Hill, Nugegallaya, Sewanagala, Sri Lanka

Article History:

- received 09 March 2023
- accepted 04 March 2024

Abstract. Traffic noise mapping frequently employs Kriging, Inverse Distance Weighted (IDW), and Triangular Irregular Networks (TIN) spatial interpolations. This study uses the Henk de Kluijver noise model to evaluate the performance of spatial interpolations. Effective traffic noise mapping requires that noise observation points (Nops) be designed as 2 m grids. The upper and lower slopes function as noise barriers to reduce sound levels. Therefore, assessment of accuracy is essential for visualising noise levels in undulating and level terrain. In addition, this work gives an accurate comparison of traffic noise interpolation in undulating areas. The elements of spatial interpolations, such as the weighting factor, variogram, radius, and number of points influence the interpolation accuracy. The Kriging with a Gaussian variogram, where the radius is 5 m and the number of points is 12 demonstrates the highest level of precision. However, there is no direct relationship between accuracy validation and cross-validation. In cross-validation, however, the accuracy of the Gaussian variogram with a 7 m radius and 18 points is more accurate. In addition, this study demonstrates that Kriging is superior for extrapolating noise levels in undulating regions. Accurate visualising traffic noise levels requires a prior understanding of spatial interpolations.

Keywords: noise observation points, accuracy validation, IDW, Kriging, TIN.

 Corresponding author. E-mail: nevilvidyamane@kdu.ac.lk

 Corresponding author. E-mail: mduznir@utm.my

1. Introduction

1.1. Road traffic noise visualisation

Noise pollution is a serious environmental problem. Road traffic noise pollution is 90% of noise pollution (Iglesias-Merchan et al., 2021). Identifying traffic noise levels is vital for noise control policies (Huang et al., 2018). Collecting traffic noise levels everywhere is not a possible task in urban cities (Ridzuan et al., 2024). Therefore, calculating traffic noise levels for designed noise observation points in two-dimensional (2D) space by a proper noise equation and spatial interpolation is prime to visualise traffic noise (Mishra et al., 2018). Noise observation points are designed as grid patterns (Kurakula & Kaffer, 2008). The number of vehicles, type of vehicle, speed of the vehicle, noise absorption by air, noise reflectance by the wall and building barriers, and noise absorption by the ground impact noise levels (Gilani & Mir, 2021). Therefore, the Henk de Kluijver traffic noise model is more effective in calcu-

lating traffic noise (Ranjbar et al., 2012). According to this model, noise reduces with the distance from $10 \log(r)$; r is the distance between the noise source and the receiver point. Therefore, designing noise observation points (as 2 m intervals) with the embedding of a 2D city model is important for noise visualisation (Debnath & Singh, 2018). Most visualisation of traffic noise was conducted in flat areas (Kurakula & Kaffer, 2008). Designing noise observation points on the undulated areas is still an issue because upslopes and downslopes act as noise barriers. Therefore, designing noise observation points beyond these slope areas is not prominent (Law et al., 2011).

Inverse distance weighted (IDW), Kriging, and triangular irregular network (TIN) are widely used to interpolate traffic noise levels. Factors associated with these interpolations affect the accuracy of the interpolated surface (Stoter et al., 2007; Tang et al., 2022). The weighting factor, number of points (observed, points), and points search radius are the factors that need to be considered for the accuracy

of IDW interpolation. Not like IDW, the correlation of observed points is considered in Kriging interpolation (Wu et al., 2022). The semi-variance of observed points is mapped in the 2D coordinate system, and the model is fitted for the semi-variance. This model is called a variogram. The circular, spherical, exponential, Gaussian, and linear are the variogram in Kriging. The accuracy of the interpolated Kriging surface depends on the variogram (Van Groenigen, 2000). The number of points and variety of the observed points affect the accuracy of the TIN interpolated surface. Therefore, considering the influence factors of these spatial interpolations is vital for noise mapping. The interpolated surface should be fitted with observed points for accurate interpolation. The surface-fitting accuracy denotes cross-validation (Risk & James, 2022). Moreover, the interpolated surface is validated by sample points using the root mean square error (RMSE) (Lesieur et al., 2021). According to accuracy validation and cross-validation, we conclude which spatial interpolation technique is the best for traffic noise interpolation.

1.2. Spatial interpolation

1.2.1. IDW interpolation

The IDW method is deterministic for multivariate spatial interpolation (Tomczak, 1998; Samal et al., 2018). Based on the mathematical assumption, the value of an unknown point is calculated by the weighted average of known points considering the neighbourhood (Schneck et al., 2021). The weight is not affected by the statistical perspective of the samples (Fung et al., 2022). The weight is inversely proportional to the distance as the value is computed as the following Equation (1) (Fung et al., 2022).

$$w(x, y) = \sum_{i=0}^N i w_i; \quad i = d_i^p / \sum_{i=1}^N d_k^p, \quad (1)$$

where: $w(x, y)$ is the predicted value positioned at the point (x, y) , N is the number of known points (x, y) , k_i is the weight of the observational results w_i positioned at the point (x_i, y_i) , d_i is the distance between the known point (x_i, y_i) and the unknown point (x, y) . Degree p is the weighting factor. The value p can be changed depending on the user's requirements. Generally, the default value of p is 2. Many geoscience problems involve predicting attribute values to unknown points. In that case, IDW is a comparative solution. However, IDW does not provide favourable results for clustered data (Chen & Liu, 2012). Compared with other spatial interpolation methods, like Kriging, the IDW does not associate with the semi-variogram model (spatial autocorrelation of the known sample points). Moreover, IDW is better for small size of samples where variograms are difficult to fit (Varentsov et al., 2020).

The influence of the weighting parameters and the number of points is considered for the interpolation, and selecting the sample points through a variable search radius and a fixed search radius are the main components used in the IDW function (Maleika, 2020). The weighting parameter shows a significant relationship between the

known values and the interpolated values. Increasing the weighting factor proportionally relates to the smoothness of the interpolated surfaces. It means that the value of the interpolated location is more the same as the value of known locations. Therefore, the weighting factor of the IDW function is vital. This is a reason for the less accurate interpolated surface. When selecting faraway known points for interpolation, the correlation between predicted points and known points may be decreased. The many numbers of known points may be a reason to get an average value for the interpolated points. Therefore, the search radius of the points is important (Maleika, 2020). Recently, IDW has been used for traffic noise mapping (Kurakula & Kaffer, 2008; Harman et al., 2016). The suggestions of these studies have recommended that the comparison of the accuracy is vital with the influence factors of the IDW for noise mapping.

1.2.2. Kriging spatial interpolation

Kriging interpolation is based on geostatistical methods that include autocorrelation (Aumond et al., 2018). Kriging is favourable for clustered data and large sizes. Kriging is not only dependent on surrounding points like IDW (Lesieur et al., 2021). It considers the autocorrelation (Fitting a model) of neighbour points. Kriging also includes an inverse distance-weighted method (Taghizadeh et al., 2013). But this weight is not only dependent on the distance between the predicted points and the observed points, and autocorrelation of observed points affects the weights. The autocorrelation is measured by semi-variance (decreasing similarity of interpolated points with observed points with distance). Ordinary Kriging is widely used for geoscience applications (Susanto et al., 2021). Assuming a constant mean for the observed points is a reasonable point of view in ordinary Kriging. Because smaller grid sizes (2 m) for noise observation points are used in traffic noise mapping, it is not an issue to apply ordinary Kriging to traffic noise mapping (Kurakula & Kaffer, 2008). Moreover, traffic noise is reduced by approximately 1dB(A) for a 2 m distance while noise propagation (Ranjbar et al., 2012). Therefore, the constant mean for the observed value (noise observation points) is a possible point of view in noise mapping. The function of Kriging is described in Equation (2) (Fazio & Roisenberg, 2013).

$$z(s_0) = \sum_{i=0}^N \lambda_i z(s_i), \quad (2)$$

where: s_0 is the predicted point, $z(s_i)$ is the measured value (known point), λ_i is the unknown weight of the measured value and N is the number of measured values (Fazio & Roisenberg, 2013). Thus, in ordinary Kriging, the model λ_i depends on the fitted model to the semi-variogram. Five fitted models for semi-variance are described in the Kriging as circular, spherical, exponential, Gaussian, and linear. These are called variograms in Kriging. The selected model influences the accuracy of the interpolated surface. Therefore, identifying a proper semi-variogram model is vital for interpolation (Van Groenigen, 2000). The following

Figure 1 illustrates the model fitting for the semi-variance in the 2D Cartesian system.

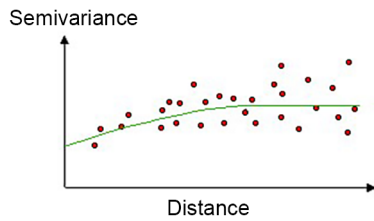


Figure 1. Model of, Variogram (Esri, 2021)

According to the graph above, it can be concluded that the correlation of points decreases with distance. There are significant equations to fit the model for the variogram (circular, spherical, exponential, Gaussian, and linear) (Jaman & Adhikary, 2020). Figures 2, 3, 4, 5, and 6 have described the shapes and equations of the mathematical models used to describe the semi-variance. In the spherical model, the spatial correlation decreases (increases the semi-variance) equivalently until some fixed distance, and then the semi-variance is a constant. In the circular model, the spatial correlation decreases until to a fixed distance, and then the semi-variance is a constant. Semi-variance increases exponentially with the distance, and it is increasing until there is an infinite distance. In the Gaussian model, semi-variance increases as concave up to a certain distance, and then increases as concave down, and semi-variance is constant finally constant. Semi-variance increases gradually in the linear model (Ramadhan et al., 2021). If the sample locations have distances closer distances to the range, these are autocorrelated (Taharin & Roslee, 2021). Therefore, to identify the accuracy of the interpolated surface by Kriging, the variogram, the number of observed points, and the range (search radius) are vital (Van Huynh et al., 2022).

1.2.3. TIN spatial interpolation

The Triangular Irregular Network (TIN) is a data structure managed to make a digital elevation model (DEM) to highly variable data (Kurakula et al., 2007). Although TIN spatial interpolation is not widely used in noise mapping, several studies were associated with TIN for interpolating of traffic noise levels (Laxmi et al., 2019). TIN provides a surface of vector-based formed by triangulating vertices (points). Collecting these serious edges that create a network of triangles. The Delaunay triangle is commonly used to create these triangles. The nothing vertex lies inside any of the triangle circumstances, and minimum interior triangles are the satisfaction for the Delaunay triangle. Because nodes can be placed irregularly on a surface, TIN has a higher visual resolution in areas where the surface is highly variable or where more details are needed. TIN is more effective at generating a continuous surface using discrete points and line data. Noise is a discrete phenomenon (Suthanaya, 2015). Therefore, it is not an issue to use the TIN to

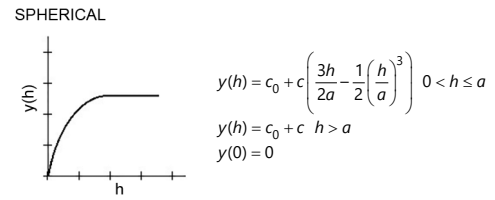


Figure 2. Spherical equation (Esri, 2021)

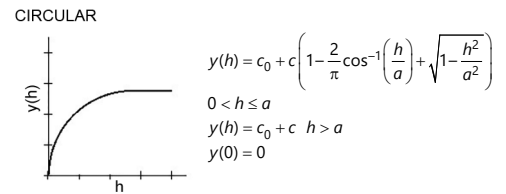


Figure 3. Circular equation (Esri, 2021)

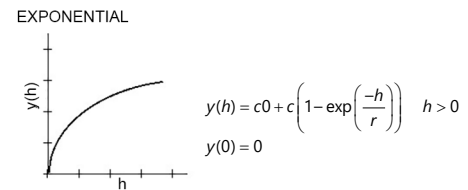


Figure 4. Exponential equation (Esri, 2021)

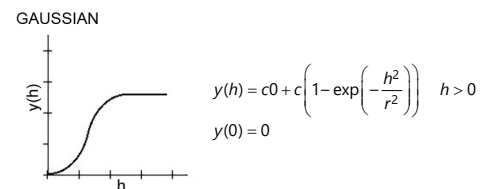


Figure 5. Gaussian equation (Esri, 2021)

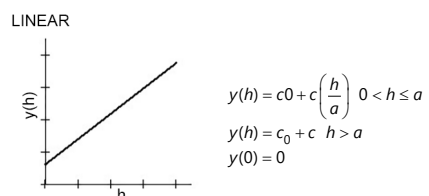


Figure 6. Linear equation (Esri, 2021)

interpolate noise levels (Wenzhong, 2000; Laxmi et al., 2019). TIN provides a facility to convert a TIN surface to a raster format through the natural neighbour (laaly-sankari et al., 2010). According to results of previous studies, traffic noise levels do not fluctuate more, and approximately 1dB(A) decreases within a distance of 2 m. However, there is some fluctuation in noise levels in the undulated areas, because upward and downward slopes appear as noise barriers. The heights of the noise observation points vary in undulated areas with road level. Therefore, applying TIN interpolation for these conditions is vital for an accurate comparison of noise mapping.

2. Methodology

2.1. Study area

The study area is located at the Universiti Teknologi Malaysia (UTM), Johor, Malaysia. The location is 1°33'37.6" N 103°38'16.4" E. There is a higher traffic flow at UTM in the morning and evening. The average traffic noise levels have been detected about 70 dB(A) (Nejad et al., 2019). This study is carried out to visualise traffic noise in 2D, space and to identify the performance of spatial interpolations on traffic noise levels. Figure 7 illustrates the overview of the study area.



Figure 7. Overview of the study area (source: Google Earth)

2.2. Methods

Digital data layers were organised to create the 2D model of the study area (buildings and road network). TIN was prepared for the terrain to identify the topographical

variance of the terrain. The TIN of the terrain is vital to identify with of the receiver (observation points) heights respect to the road level. The research workflow is shown in Figure 8. Noise observation points (Nops) were designed as normal to the centreline of the roads, and maintained 2 m distance intervals a pair of Nops. The number of vehicles and the speed of vehicles (road statistical data) were observed in the morning (7.30 a.m. to 9.30 a.m.). The Henk de Kluijver traffic noise model was used to calculate noise levels to Nops. Equation (3) elaborates on the Henk de Kluijver traffic noise model (Ranjbar et al., 2012).

$$L_{Aeq} = E + C_{optrek} + C_{reflectie} - D_{afstand} - D_{lucht} - D_{bodem} - D_{meteo} - D_{barrier} \quad (3)$$

L_{Aeq} is the noise level of the Nop, and E is the noise emission level. C_{optrek} is the extra noise emission from vehicle braking and accelerating. $C_{reflectie}$ is the noise reflexion of barriers. The $D_{afstand}$ is the mitigation of traffic noise with distance. D_{lucht} is the mitigation of traffic noise due to absorption from the air. r is the shortest distance between the noise source and the observation point. D_{bodem} is the traffic noise absorption by the ground. D_{meteo} denotes the reduction in noise caused by wind conditions. The noise reflexion correction was determined as +1.5 dB(A). When the ground is completely made up of grass, the noise absorption coefficient of the ground was assumed to be 1 (International Organization for Standardization, 1996). Then the noise absorption coefficient

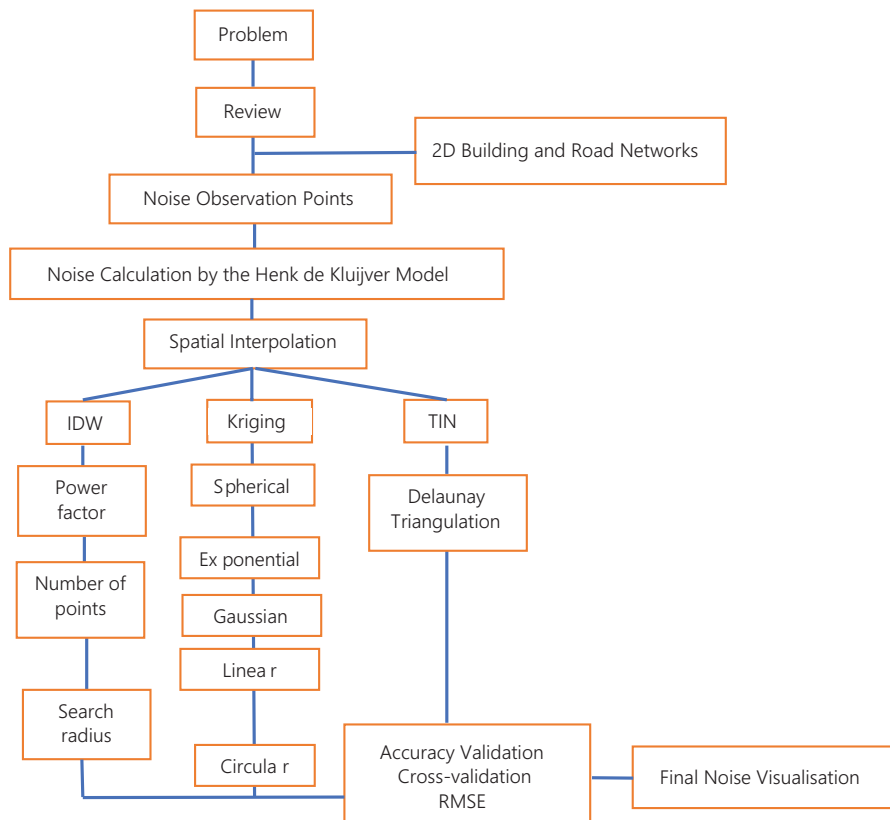


Figure 8. Research workflow

of ground was assumed to be 0.7 for lawns, and 0.3 for gravel roads (Attenborough et al., 2016). The samples points were randomly selected to validate the interpolated surface. The grid resolution was considered to be 1 m for the interpolated surface. In the IDW, the power parameter was selected as 1, 2, 3, and 4. The number of points and selecting observation points through the variable search radius were fixed as respectively 6, 8, and 12, 3 m, 5 m, and 7 m. In the Kriging, different types of variogram were used for the interpolation, and the Delaunay triangulation method was used for the TIN. An accuracy comparison was conducted through a cross-validation (fitting observation points with interpolated surface) and a sample validation (to validate the interpolated surfaces with sample points). Especially, the accuracy validation of the interpolated surface was carried out for the entire study area and slope areas separately to obtain a significant comparison of the interpolated surface.

3. Results and discussion

Figure 9 illustrates the Nops and 2D model of the study area. The hundred (100) sample noise observations were used to validate interpolated surfaces. Sample points were selected by considering the density of sample points, the number of samples, and distribution of samples with respect to the study area. The forty (40) Nops were used for cross-validation. Table 1 and Figure 10 show the accuracy comparison of the IDW interpolation. In Figure 10, 1, 2, 3, 4, and 5 refers to the weighting factor. Table 2 and Figure 11 show the accuracy comparison of the Kriging interpolation.

Table 1. Accuracy validation of IDW

Radius	Points	Power (1)	Power (2)	Power (3)	Power (4)	Power (5)
3	6	2.633	2.628	2.708	2.807	2.892
5	12	2.828	2.580	2.584	2.690	2.795
7	18	3.188	3.024	3.102	3.157	3.055

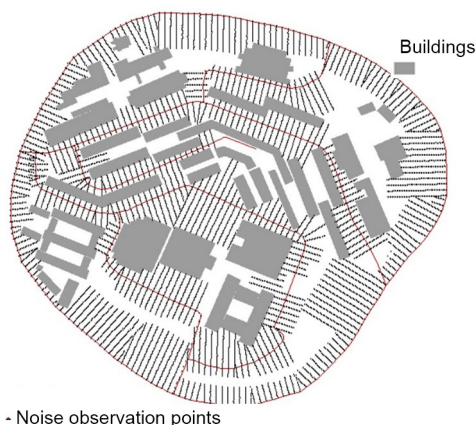


Figure 9. 2D Model with nops

Table 2. Accuracy validation of Kriging

Radius, Points	Spherical (1)	Circle (2)	Exponential (3)	Gaussian (4)	Linear (5)
3,6	2.071	2.107	1.893	21.431	2.204
5,12	1.747	1.731	1.677	1.529	1.734
7,18	1.741	1.730	1.682	1.549	1.709

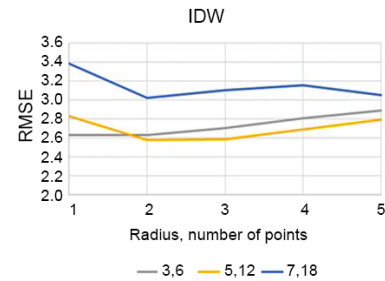


Figure 10. Accuracy validation of IDW

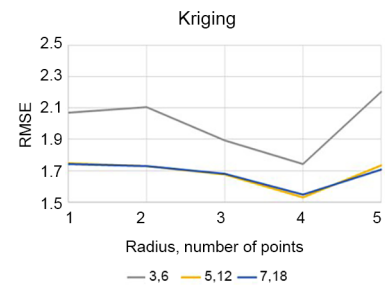


Figure 11. Accuracy validation of Kriging

According to Table 1, the weighting factor of IDW is 1,2,3,4, and 5. The number of points and fixed radius have been used for the interpolations that show in the first and second columns. According to Figure 10, the minimum RMSE (2.580) is represented for the weighting factor is 2, the number of points is 12, and the distance of the radius is 5 m in IDW interpolation. According to Table 2 and Figure 11, the minimum RMSE (1.529) is represented for the Gaussian variogram, and the radius and number of points are respectively, 5 m and 12. However, the minimum RMSE for IDW and Kriging was taken when the number of points is 12 and the fixed radius distance is 5 m. It means that when distance between Nops is 2 m, the number of points is 12 and the fixed radius is 5 m is vital for the accuracy of IDW and Kriging interpolation. The RMSE is closed together when weighting factor is 5, whatever fixed radius and number of points in IDW interpolation. In Kriging, the minimum RMSE is taken for the Gaussian variogram whatever fixed radius and number of points. The RMSE of accuracy validation for TIN is 3.341. Therefore, the type of variogram and the weighting factor of the Kriging and IDW is vital for the accuracy of the interpolated surface.

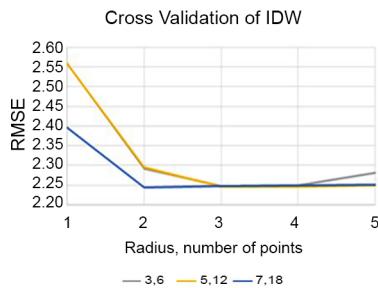
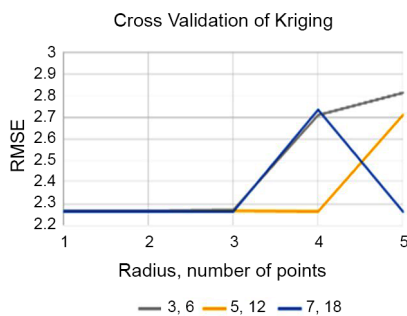
For cross-validation (to identify the accuracy comparison of the interpolated surface and Nops), the 40 Nops were used to find the RMSE between Nops and the

Table 3. Cross-validation of IDW

Radius	Points	Power (1)	Power (2)	Power (3)	Power (4)	Power (5)
3	6	2.560	2.292	2.247	2.249	2.281
5	12	2.559	2.295	2.246	2.247	2.249
7	18	2.396	2.244	2.247	2.250	2.251

Table 4. Cross-validation of Kriging

Radius, Points	Spherical (1)	Circle (2)	Exponential (3)	Gaussian (4)	Linear (4)
3,6	2.268	2.267	2.270	2.711	2.811
5,12	2.266	2.265	2.265	2.265	2.711
7,18	2.267	2.265	2.263	2.733	2.264

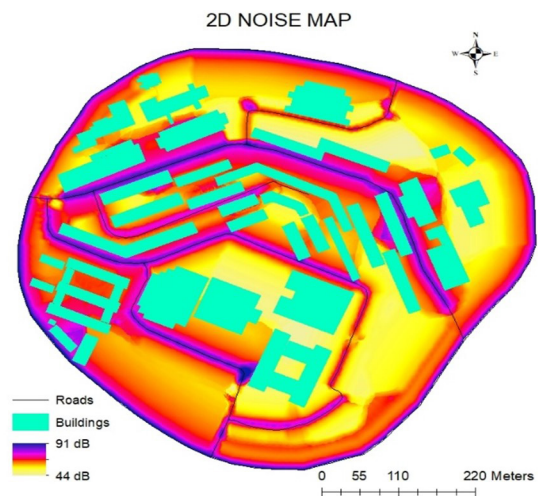
**Figure 12.** Cross-validation of IDW**Figure 13.** Cross-validation of Kriging

interpolated surface. According to Table 3 and Figure 12, the minimum RMSE was taken when the weighting factor is 2, radius 7, and the number of points is 18 in IDW. Thus, it can be concluded that RMSE is minimised for both accuracy validation and cross-validation when the weighting factor of IDW is 2. However, when the weighting factor is applied, the accuracy of cross-validation is increased in IDW. In Kriging interpolation, Table 4 and Figure 13 there are no a direct relationship between accuracy and interpolation factors. But the accuracy of cross-validation is higher in the Gaussian variogram. The RMSE for cross-validation of TIN is 3.443. The 20 sample noise points were selected to validate the noise levels in undulated areas. Table 5 shows the accuracy validation of Kriging, IDW, and TIN noise interpolations in undulated areas.

Table 5. Accuracy validation of undulated areas

	Kriging	IDW	TIN
RMSE	1.690	3.017	4.321

The IDW surface with RMSE is 2.580 was used to validate sample points in undulated areas. Like that, a Kriging surface was used, which RMSE is 1.529. The similar TIN surface mentioned above was used. However, the Kriging interpolation has a lower RMSE in undulated areas. But comparatively, there is a higher RMSE for IDW, and TIN in undulated areas. When considering the accuracy of Kriging, IDW and TIN interpolated surfaces, the Kriging (Gaussian variogram, radius is 5 m, and number of points is 12) has a lower RMSE than other interpolated surfaces. Therefore, to visualise the 2D noise levels, this Kriging surface was used. The 2D traffic noise visualisation is shown in Figure 14.

**Figure 14.** Visualisation of 2D traffic noise

4. Conclusions

A proper noise model is vital for the calculation of traffic noise. Visualisation of traffic noise is effective in designing noise policies for urban planners. Although IDW, Kriging, and TIN are widely used to interpolate traffic noise levels, the performance of spatial interpolations is vital for noise mapping. The Gaussian variogram of Kriging (with radius is 5 m and number of points are 12) is prime to increase the accuracy of interpolated surface. However, to achieve that much accuracy, the distance should be maintained at 2 m between Nops. In cross-validation (fitting interpolated surface with Nops), the IDW (weighting factor is 2, radius is, 7 and number of points are 18) has a high accuracy. However, there is no direct relationship between cross-validation and accuracy validation of traffic noise interpolated surfaces. In undulate areas, the Kriging shows a higher accuracy for traffic noise interpolation. Therefore, Kriging is vital to interpolate traffic noise levels under any topographical conditions. The Kriging considers the cor-

relation between observation points, the values of Nops, not more variety. Therefore, the Kriging spatial interpolation technique fits to sample points with higher accuracy.

References

- Attenborough, K., Bashir, I., & Taherzadeh, S. (2016). Exploiting ground effects for surface transport noise abatement. *Noise Mapping*, 3(1), 1–25. <https://doi.org/10.1515/noise-2016-0001>
- Aumond, P., Can, A., Mallet, V., De Coensel, B., Ribeiro, C., Botteldooren, D., & Lavandier, C. (2018). Kriging-based spatial interpolation from measurements for sound level mapping in urban areas. *The Journal of the Acoustical Society of America*, 143(5), 2847–2857. <https://doi.org/10.1121/1.5034799>
- Chen, F. W., & Liu, C. W. (2012). Estimation of the spatial rainfall distribution using inverse distance weighting (IDW) in the middle of Taiwan. *Paddy and Water Environment*, 10(3), 209–222. <https://doi.org/10.1007/s10333-012-0319-1>
- Debnath, A., & Singh, P. K. (2018). Environmental traffic noise modelling of Dhanbad township area – A mathematical based approach. *Applied Acoustics*, 129, 161–172. <https://doi.org/10.1016/j.apacoust.2017.07.023>
- Esri. (2021). *ArcGIS Desktop*.
- Fazio, V. S., & Roisenberg, M. (2013). Spatial interpolation: An analytical comparison between Kriging and RBF networks. *Proceedings of the ACM Symposium on Applied Computing*, 2(1), 2–7. <https://doi.org/10.1145/2480362.2480364>
- Fung, K. F., Chew, K. S., Huang, Y. F., Ahmed, A. N., Teo, F. Y., Ng, J. L., & Elshafie, A. (2022). Evaluation of spatial interpolation methods and spatiotemporal modelling of rainfall distribution in Peninsular Malaysia. *Ain Shams Engineering Journal*, 13(2), Article 101571. <https://doi.org/10.1016/j.asej.2021.09.001>
- Gilani, T. A., & Mir, M. S. (2021). Modelling road traffic noise under heterogeneous traffic conditions using the graph-theoretic approach. *Environmental Science and Pollution Research*, 28(27), 36651–36668. <https://doi.org/10.1007/s11356-021-13328-4>
- Harman, B. I., Koseoglu, H., & Yigit, C. O. (2016). Performance evaluation of IDW, Kriging and multiquadric interpolation methods in producing noise mapping: A case study at the city of Isparta, Turkey. *Applied Acoustics*, 112, 147–157. <https://doi.org/10.1016/j.apacoust.2016.05.024>
- Huang, Y., Wang, L., Hou, Y., Zhang, W., & Zhang, Y. (2018). A prototype IOT based wireless sensor network for traffic information monitoring. *International Journal of Pavement Research and Technology*, 11(2), 146–152. <https://doi.org/10.1016/j.ijprt.2017.07.005>
- laaly-sankari, A., Jadayel, O., & El-murr, N. (2010). Urban Noise Mapping: The Case of the City of El-Mina, North Lebanon. In *Proceedings Middle East & North Africa Users Conference ESRI* (p. 10).
- Iglesias-Merchan, C., Laborda-Somolinos, R., González-Ávila, S., & Elena-Rosselló, R. (2021). Spatio-temporal changes of road traffic noise pollution at ecoregional scale. *Environmental Pollution*, 286, Article 11729. <https://doi.org/10.1016/j.envpol.2021.117291>
- International Organization for Standardization. (1996). *Acoustics – attenuation of sound propagation outdoors* (ISO Standard No. 9613-2:1996).
- Jaman, N. I., & Adhikary, S. K. (2020, February). A positive Kriging approach for missing rainfall estimation. In *The 5th International Conference on Civil Engineering for Sustainable Development* (pp. 1–10). https://www.researchgate.net/publication/340447627_A_Positive_Kriging_Approach_for_Missing_Rainfall_Estimation
- Kurakula, V. K., & Kuffer, M. (2008). 3D noise modelling for urban environmental planning and management. In *Real Corp 0088: Mobility Nodes as Innovation Hubs* (pp. 517–523). https://www.researchgate.net/publication/228622472_3D_Noise_Modeling_for_Urban_Environmental_Planning_and_Management
- Kurakula, V., Skidmore, A., Kluijver, H. D., Stoter, J., Dąbrowska-Zielińska, K., & Kuffer, M. (2007). A GIS-Based approach for 3D noise modelling using 3D city models. *International Institute for Geo-Information Science and Earth*, 319(5864), 766–769. <https://www.semanticscholar.org/paper/A-GIS-Based-approach-for-3D-noise-modelling-using-Kurakula-Skidmore/0a3e4950ec0e7ec852b90c444d66e4618757a75b>
- Law, C. W., Lee, C. K., Lui, A. S. W., Yeung, M. K. L., & Lam, K. C. (2011). Advancement of three-dimensional noise mapping in Hong Kong. *Applied Acoustics*, 72(8), 534–543. <https://doi.org/10.1016/j.apacoust.2011.02.003>
- Laxmi, V., Dey, J., Kalawapudi, K., Vijay, R., & Kumar, R. (2019). An innovative approach of urban noise monitoring using cycle in Nagpur India. *Environmental Science and Pollution Research. Environmental Science and Pollution Research*, 26(36), 36812–36819. <https://doi.org/10.1007/s11356-019-06817-0>
- Lesieur, A., Mallet, V., Aumond, P., & Can, A. (2021). Data assimilation for urban noise mapping with a meta-model. *Applied Acoustics*, 178, Article 107938. <https://doi.org/10.1016/j.apacoust.2021.107938>
- Maleika, W. (2020). Inverse distance weighting method optimization in the process of digital terrain model creation based on data collected from a multibeam echosounder. *Applied Geomatics*, 12(4), 397–407. <https://doi.org/10.1007/s12518-020-00307-6>
- Mishra, R. K., Mishra, A. R., & Singh, A. (2018). Traffic noise analysis using RLS-90 model in urban city. *Inter-Noise and Noise- Congress and Conference Proceedings*, 13, 6490–6502.
- Nejad, P. G., Ahmad, A., & Zen, I. S. (2019). Assessment of the Interpolation techniques on traffic noise pollution mapping for the campus environment sustainability. *International Journal of Built Environment & Sustainability*, 6(1–2), 147–159. <https://doi.org/10.11113/ijbes.v6.n1-2.393>
- Ramadhan, M. D., Marwanza, I., Nas, C., Azizi, M. A., Dahani, W., & Kurniawati, R. (2021). Drill holes spacing analysis for estimation and classification of coal resources based on variogram and Kriging. *IOP Conference Series: Earth and Environmental Science*, 819(1), Article 012026. <https://doi.org/10.1088/1755-1315/819/1/012026>
- Ranjbar, H. R., Gharagozlou, A. R., & Vafaei Nejad, A. R. (2012). 3D analysis and investigation of traffic noise impact from Hemmat Highway located in Tehran on buildings and surrounding areas. *Journal of Geographic Information System*, 4(4), 322–334. <https://doi.org/10.4236/jgis.2012.44037>
- Risk, C., & James, P. M. A. (2022). Optimal cross-validation strategies for selection of spatial interpolation models for the Canadian forest fire weather index system. *Earth and Space Science*, 9(2), 1–17. <https://doi.org/10.1029/2021EA002019>
- Ridzuan, N., Wickramathilaka, N., Ujang, U., & Azri, S. (2024). 3D voxelisation for enhanced environmental modelling applications. *Pollution*, 10(1), 151–167. <https://doi.org/10.22059/poll.2023.360562.1942>
- Samal, K., Babu, K., & Das, S. (2018). Spatio-temporal prediction of air quality using distance-based interpolation and deep learning techniques. *EAI Endorsed Transactions on Smart Cities*, 5(14), Article 168139. <https://doi.org/10.4108/eai.15-1-2021.168139>
- Schneck, T., Telbisz, T., & Zsuffa, I. (2021). Precipitation interpolation using digital terrain model and multivariate regression in

- hilly and low mountainous areas of Hungary. *Hungarian Geographical Bulletin*, 70(1), 35–48.
<https://doi.org/10.15201/hungeobull.70.1.3>
- Susanto, A., Setyawan, D. O., Setiabudi, F., Savira, Y. M., Listiari, A., Putro, E. K., Muhamad, A. F., Wilmot, J. C., Zulfakar, D., Kara, P., Shofwati, I., Sodikin, S., & Tejamaya, M. (2021). GIS-based mapping of noise from mechanized minerals ore processing industry. *Noise Mapping*, 8(1), 1–15.
<https://doi.org/10.1515/noise-2021-0001>
- Suthanaya, P. A. (2015). Modelling road traffic noise for collector road (case study of Denpasar City). *Procedia Engineering*, 125, 467–473. <https://doi.org/10.1016/j.proeng.2015.11.125>
- Stoter, J. E., Kluijver, H. De., & Kurakula, V. (2007). *3D noise contours*. <https://www.dbvision.nl/bestanden/overons/publicaties/2007/20071106%20Stoter%20dr.%20J.E.,%20Kluijver%20ir.%20H.%20de,%20Kurakula%20V.,%203.pdf>
- Taghizadeh, R., Zare, M., & Zare, S. (2013). Mapping of noise pollution by different interpolation methods in recovery section of Ghandi telecommunication Cables Company. *Journal of Occupational Health and Epidemiology*, 2(1), 1–11.
<https://doi.org/10.18869/acadpub.johe.2.1.2.1>
- Taharin, M. R., & Roslee, R. (2021). The application of semi variogram and ordinary Kriging in determining the cohesion and clay percentage distribution in hilly area of Sabah, Malaysia. *International Journal of Design and Nature and Ecodynamics*, 16(5), 525–530. <https://doi.org/10.18280/ijdne.160506>
- Tang, J. H., Lin, B. C., Hwang, J. S., Chen, L. J., Wu, B. S., Jian, H. L., Lee, Y. T., & Chan, T. C. (2022). Dynamic modeling for noise mapping in urban areas. *Environmental Impact Assessment Review*, 97, Article 106864.
<https://doi.org/10.1016/j.eiar.2022.106864>
- Tomczak, M. (1998). Spatial interpolation and its uncertainty using automated anisotropic Inverse Distance Weighting (IDW)-Cross-validation/Jackknife Approach. *Journal of Geographic Information and Decision*, 2(2), 18–30.
- Van Groenigen, J. W. (2000). The influence of variogram parameters on optimal sampling schemes for mapping by kriging. *Geoderma*, 97(3–4), 223–236.
[https://doi.org/10.1016/S0016-7061\(00\)00040-9](https://doi.org/10.1016/S0016-7061(00)00040-9)
- Van Huynh, C., Pham, T. G., Nguyen, L. H. K., Nguyen, H. T., Nguyen, P. T., Le, Q. N. P., Tran, P. T., Nguyen, M. T. H., & Tran, T. T. A. (2022). Application GIS and remote sensing for soil organic carbon mapping in a farm-scale in the hilly area of central Vietnam. *Air, Soil and Water Research*, 2022, Article 15. <https://doi.org/10.1177/11786221221114777>
- Varentsov, M., Esau, I., & Wolf, T. (2020). High-resolution temperature mapping by geostatistical kriging with external drift from large-eddy simulations. *Monthly Weather Review*, 148(3), 1029–1048. <https://doi.org/10.1175/MWR-D-19-0196.1>
- Wenzhong, S. (2000). Development of a hybrid model for three dimensional GIS. *Geospatial Information Science*, 3(2), 6–12.
<https://doi.org/10.1007/BF02826617>
- Wu, S., Fu, F., Wang, L., Yang, M., Dong, S., He, Y., & Zhang, Q. (2022). Short-term regional temperature prediction based on deep spatial and temporal networks. *Atmosphere*, 13(12), Article 1948. <https://doi.org/10.3390/atmos13121948>